Letter

Electric polarization and its quantization in one-dimensional non-Hermitian chains

Jinbing Hu,[1,2,*] Carmine Antonio Perroni,[2,†] Giulio De Filippis,[2] Songlin Zhuang,[1] Lorenzo Marrucci,[2] and Filippo Cardano[2]

[1]*College of Optical-Electrical Information and Computer Engineering, University of Shanghai for Science and Technology, Shanghai 200093, China*

[2]*Dipartimento di Fisica "Ettore Pancini", Università degli Studi di Napoli Federico II, Complesso Universitario di Monte Sant'Angelo, Via Cintia, 80126 Napoli, Italy*

(Received 19 April 2022; revised 14 November 2022; accepted 13 February 2023; published 10 March 2023)

We generalize the modern theory of electric polarization to the case of one-dimensional (1D) non-Hermitian systems with a line-gapped spectrum. In these systems, the electronic position operator is non-Hermitian even when projected into the subspace of states below the energy gap. However, in the framework of biorthogonal quantum mechanics, the associated Wilson-loop operator is unitary in the thermodynamic limit, thereby leading to real-valued electronic positions that allow for a clear definition of polarization. Non-Hermitian polarization can be quantized in the presence of certain symmetries, as for Hermitian insulators. Differently from the latter case, however, in this regime polarization quantization depends also on the type of energy gap, which can be either real or imaginary, leading to a richer variety of topological phases. The most counterintuitive example is the 1D non-Hermitian chain with time-reversal symmetry only, where non-Hermitian polarization is quantized in the presence of an imaginary-line gap. We propose two specific models to provide numerical evidence supporting our findings.

DOI: 10.1103/PhysRevB.107.L121101

Although the concept of electric polarization was introduced 100 years ago [1], it was not until the early of 1990s that the long-standing problem of crystalline polarization was solved [2–6]. The main reason is that in a crystalline material the macroscopic polarization cannot be unambiguously defined as the dipole of a unit cell, since *the electronic wave functions are delocalized over the whole lattice*. The first step towards a theory of polarization was made by Resta [2], who cast the polarization difference as an integrated macroscopic current. Since then, King-Smith and Vanderbilt [3] immediately built what is now known as the modern theory of polarization of crystalline insulators, which shows that the bulk polarization is strictly related to electronic geometric phases [7–9]. When the lattice Hamiltonian obeys inversion and/or chiral symmetry (IS and/or CS), the polarization is quantized. Nonvanishing values of the *bulk* polarization are associated with the appearance of *boundary* charges [10], according to the so-called bulk-boundary correspondence (BBC) [11–13], a hallmark of topological physics.

When electrons in a crystalline insulator interact with the environment, their effective dynamics is described through a non-Hermitian (NH) Hamiltonian [14]. Enormous attention is currently devoted to NH physics, which is rich in unconventional phenomena such as unidirectional invisibility [15–17], exceptional-point encirclement [18–20], enhanced sensitivity [21–23], and the NH skin effect [24–27]. These phenomena have been reproduced in a variety of artificial simulators [28–31].

Within this extremely active research field, little is known about NH electric polarization. Very recently, three papers discussed NH polarization by means of many-body wave functions [32], entanglement spectrum [33], and generalizing Resta's formula using a biorthogonal basis [34]. Similar to the Hermitian case, these approaches considered only systems having chiral and/or inversion symmetries. However, non-Hermiticity is known to alter dramatically the definition of internal symmetries due to the distinction of complex conjugation and transposition [35,36], and to present different types of energy gaps [36]. As such, it is crucial to understand if NH polarization is quantized in a larger variety of configurations, compared to the Hermitian case, and how these conditions are related to the type of energy gap.

In this Letter we provide a generalization of the standard theory of electric polarization [3] to line-gapped NH systems, where the bulk wave functions are extended across the entire system, such as those of Hermitian crystalline materials, and the identification of a ground state is not ambiguous [33]. We follow a traditional approach, relying on the projection of the electronic position operator into a subspace of single-particle wave functions that fill the bands below the gap [10]. Although the projected position operator is itself non-Hermitian, we find that it leads to a unitary Wilson-loop operator. Therefore, the Wannier centers [37], i.e., the phases of Wilson-loop eigenvalues, are purely real valued, and so is the electric polarization, which is the summation of Wannier centers [10]. Wilson-loop operators and related eigenvalues have already proved key to the definition of topological invariants of NH

*hujinbing@usst.edu.cn
†carmine.perroni@unina.it

systems [38,39] and edge polarization in two-dimensional (2D) lattices [40]. Compared to other approaches [32–34], our derivation allows us to analyze systematically the restrictions of the basic symmetries to the Wilson-loop operator in systems with either real- or imaginary-line gaps, obtaining in turn the quantization conditions of NH polarization. With respect to the Hermitian case, we find that NH systems host a larger number of topological phases, which are protected by both symmetries and type of energy gap. The electric polarization studied here is conceptually different from the biorthogonal polarization introduced in Ref. [41], which represents a topological invariant defined in terms of zero-energy modes under open boundary conditions.

Let us start by considering a one-dimensional (1D) NH crystalline chain composed of N unit cells, each made of $N_{\rm orb}$ lattice sites or orbitals. In this system, the electric polarization can be computed in a single unit cell as the dipole moment density, that is, $p = -\frac{1}{a}\sum_{\alpha=1}^{N_{\rm elec}} e\, r_\alpha$, where $N_{\rm elec} < N_{\rm orb}$ is the number of electrons in each unit cell, a is the lattice spacing, e is the absolute value of the electron charge, and r_α's are the electron positions with respect to the center of positive charges in the cell. More details can be found in the Supplemental Material (SM) [42] (see also Refs. [43–49] therein). For simplicity, we set $a = e = 1$. The modern theory of electric polarization provides an elegant method to determine positions r_α in quantum systems where bulk electrons are delocalized, starting from the position operator projected into the subspace of occupied bands [10]. A straightforward definition of the position operator is $\hat{x} = \sum_{j=1}^{N}\sum_{\alpha=1}^{N_{\rm orb}} \hat{x}_{j,\alpha}$, where $\hat{x}_{j,\alpha} = (j + x_\alpha)\hat{c}^\dagger_{j,\alpha}|0\rangle\langle 0|\hat{c}_{j,\alpha}$, with $\hat{c}^\dagger_{j,\alpha}$ ($\hat{c}_{j,\alpha}$) the creation (annihilation) operators for electrons within cell j and orbital α, x_α the position of the orbital α within the unit cell, and $|0\rangle$ the vacuum state for the electrons. Unfortunately, $\hat{x}$ is not a legitimate operator for finite values of N when periodic boundary conditions (PBCs) are used. To overcome this, a unitary position operator was proposed [5,50], i.e., $\hat{x}_e = \exp(i2\pi\hat{x}/N)$. This operator is defined modulo N, thus obeying PBC. Let us note that such an operator was originally discussed when considering its expectation value [5]. However, in Ref. [51] the authors showed that this definition has to be corrected, in case one is willing to compute the distance of two coordinates, not its average value. Importantly, in the case of independent and noninteracting electrons, such as our situation, both approaches give the same outcome, hence we can safely use the unitary operator $\hat{x}_e$ defined above.

By discrete Fourier transformation, $\hat{x}_e$ can be alternatively written in momentum space as [42]

$$\hat{x}_e = \sum_{k,\alpha} \hat{c}^\dagger_{k+\Delta k,\alpha}|0\rangle\langle 0|\hat{c}_{k,\alpha}, \tag{1}$$

where $k \in \Delta k \cdot (0, 1, \ldots, N-1)$, $\Delta k = 2\pi/N$, and $\hat{c}^\dagger_{k,\alpha}$ ($\hat{c}_{k,\alpha}$) are creation (annihilation) operators for electrons with momentum k in the orbital α.

On the basis of position operator Eq. (1), the projected position operator can be achieved by projecting it into the subspace of electronic states that are occupied [10]. In the Hermitian case, these are typically obtained by looking at the band structure and considering all states whose energy is below the Fermi energy. However, this procedure is more subtle in NH systems, where eigenenergies are normally complex and can be arranged in bands exhibiting three types of energy gap (see Fig. 1), that is, a point gap, a real-line gap, and an imaginary-line gap. The first is associated with NH skin effect [24–27], where the wave functions of single-particle eigenstates are all localized at the boundary the system and the definition of occupied states is ambiguous [33]. A theory of the electric polarization for this system has been successfully proposed by relying on a many-body approach, showing essentially that owing to the Pauli exclusion principle the many-body eigenstates are delocalized in the bulk of the system [32]. An alternative formulation has been recently proposed in Ref. [33] in terms of single-particle states, yet the obtained polarization is complex valued when the spectrum is point gapped. Here, we preferred not the deal with these ambiguities and focus on line-gapped systems only, which can be continuously deformed into (anti-)Hermitian ones while keeping the line gap and symmetry [35]. As such, occupied bands can be well defined, at least in the theoretical models. Indeed, in our discussion, we will consider as occupied those eigenstates whose energies, actually their real/imaginary parts, are below the real/imaginary-line gap, respectively (see Fig. 1). At this level the type of line gap is not playing any role (the gap could be also both real and imaginary), while it will be clearer below that conditions for quantizing the electric polarization are different in the two cases. With this in mind, the projected position operator can be written as [42]

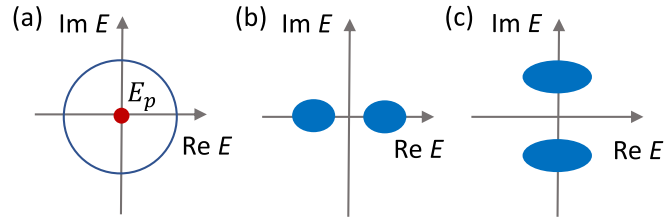

FIG. 1. Schematic for energy gaps of NH Hamiltonians. (a) In a point gap, there is a reference value E_p that is not touched by the energy bands. (b), (c) In a real/imaginary-line gap, energies are grouped in at least two bands, whose real/imaginary part is separated by a finite gap [35]. It is also possible that there is a separation of both the real and imaginary parts of the spectrum of gapped bands.

$$\hat{P}^{\rm occ}\hat{x}_e\hat{P}^{\rm occ} = \sum_{n,m=1}^{N_{\rm occ}}\sum_{k} \hat{\gamma}^R_{m,k+\Delta k}|0\rangle[G_k]^{mn}\langle 0|\hat{\gamma}^L_{n,k}, \tag{2}$$

where G_k is the core matrix defined in the Supplemental Material [42], $\hat{\gamma}^j_{n,k}(j = R/L)$ is the right/left creation/annihilation operator of electrons with quasimomentum k in the nth band, and $N_{\rm occ}$ is the number of bands whose energies are below the line gap. Equation (2) is conceptually similar to Eq. (8) in Ref. [32], where the average of the position operator is computed for the many-body ground state. Although starting from a similar expression, here we take a different path to computing the polarization, that is, the approach harnessed in Hermitian systems [10]. As we show below, this gives us the chance to obtain directly quantization conditions based on the analysis of the Wilson-loop operator.

In the circumstance of Hermitian insulators, the projected position operator is Hermitian [10]. In the NH case, however,

the operator in Eq. (2) is NH since it is constructed in terms of right and left eigenvectors of the NH Hamiltonian. At first sight, one would expect that this cannot generate real-valued Wannier centers. Nevertheless, by looking at the Wilson-loop operator, which is unitary in the thermodynamic limit as long as the right and left eigenvectors are complete, one can realize that this is not the case. Actually, for finite values of Δk, the core matrix G_k is not unitary, in analogy with the Hermitian case [10]. As discussed in the Supplemental Material [42], one can generalize the Hermitian procedure in Ref. [10] to the non-Hermitian case by introducing a singular value decomposition (SVD) [52] of the matrix G_k, $G_k = U_k D_k V_k^\dagger$, with U_k and V_k both unitary, and D_k a diagonal matrix. Indeed, the matrix $F_k = U_k V_k^\dagger$, which is unitary, can be used to construct unitary Wilson-loop operators that, in the thermodynamic limit, converge to those obtained in terms of G_k. This procedure is explicitly used to obtain accurate Wilson-loop eigenvalues.

By using the operator F_k a unitary Wilson loop [38–40,53,54] can be constructed by multiplying the latter along the Brillouin zone (BZ). As shown in Ref. [42], this converges to the one obtained in terms of G_k in the thermodynamic limit. As the Wilson-loop operator is unitary, the phases of its eigenvalues are real numbers that still define the Wannier centers, i.e., the electronic displacement with respect to the center of positive charges. Based on this implicit relation, the NH electric polarization can be extracted as

$$p = \sum_{j=1}^{N_{\rm occ}} \epsilon^j, \tag{3}$$

where ϵ^j is the phase of the Wilson-loop eigenvalue, satisfying $W_{k+2\pi\leftarrow k}|\epsilon_k^j\rangle = e^{i2\pi\epsilon^j}|\epsilon_k^j\rangle$, and $|\epsilon_k^j\rangle$ is the Wilson-loop eigenstate. In fact, the polarization defined in Eq. (3) can be expressed as the integral of complex Berry connection [55] A_k over the BZ [42],

$$p = -\frac{1}{2\pi}\oint_{\rm BZ} {\rm Tr}[A_k]dk \bmod 1, \tag{4}$$

which agrees with the well-known expression of the polarization [3–5], that is, the electric polarization is a natural topological invariant.

Quantization conditions. Symmetries play a pivotal role in quantizing electric polarization; IS, for instance, forces the polarization to be either 0 or 1/2 in Hermitian crystalline insulators [10]. In NH physics, the definition of internal symmetries are dramatically altered due to the distinction of complex conjugation and transposition [27,35]. Including pseudo-Hermiticity and inversion symmetry, there are eight basic symmetries [42], i.e., IS, CS, sublattice symmetry (SLS), time-reversal symmetry (TRS), anomalous TRS (TRS†), pseudo-Hermiticity (η-H), particle-hole symmetry (PHS), and anomalous PHS (PHS†), with related operators $I, \Gamma, S, T, \tilde{T}, \eta, C, \tilde{C}$, respectively. It is necessary to study what symmetries quantize NH polarization.

As mentioned above, Eq. (3) provides a convenient way to determine the quantization conditions of NH polarization by analyzing the restriction of symmetries to the unitary Wilson-loop operator. Going beyond previous studies, here we investigate the constraint of these basic symmetries to NH polarization, both in real and imaginary gapped systems, which are associated with different symmetry-protected topological phases [35]. The results we obtain are summarized in Table I, which clearly shows that, compared to the Hermitian case, NH polarization is quantized in a larger number of symmetry classes. The corresponding topological classes can be found in Ref. [35]. In general, the quantization conditions can be categorized into three classes: the first includes TRS† and η-H, imposing no restriction to the NH polarization; the second class includes IS, SLS, and PHS, each presenting quantized bulk polarization for both real- and imaginary-line gaps; the last class includes CS, TRS, PHS†, which quantizes NH polarization only for real- or imaginary-line gaps. Note that, for each of the last three symmetries in Table I, i.e., TRS, PHS, PHS†, the quantization condition is only applicable when the symmetry operator g satisfies $gg^* = 1 (g = T, C, \tilde{C})$, while the unitary sewing matrix is zero for $gg^* = -1 (g = T, C, \tilde{C})$ [42].

TABLE I. The quantization table of NH electric polarization for eight basic symmetries. r and i denote real-line and imaginary-line gaps, respectively, and $\surd$ indicates the quantization of bulk polarization by the corresponding symmetry. Note that for each of the last three types of symmetries, the quantization of polarization is only applicable when the symmetry operator g satisfies $gg^* = 1$ ($g = T, C, \tilde{C}$). The topological classes corresponding to these symmetries are provided in Ref. [35].

	IS	CS	SLS	TRS†	η-H	TRS	PHS	PHS†
r	$\surd$	$\surd$	$\surd$				$\surd$	$\surd$
i	$\surd$		$\surd$			$\surd$	$\surd$	

Among the cases summarized in Table I, systems with TRS and an imaginary-line gap represent a significant example, which is fully distinct with respect to the Hermitian case. In Hermitian insulators indeed, TRS imposes no restrictions to electric polarization because the energies satisfy the relation $E_\pm(k) = E_\pm(-k)$, and bands are individually subject to TRS, thus, the topological phase is absent [36]. In NH physics, however, under the constraint of TRS, the energy spectrum satisfies the relation $E_+(k) = E_-^*(-k)$. If the energy spectrum is characterized by an imaginary-line gap, then the positive and negative imaginary bands are always paired; considering the fact that the Hilbert space of all bands is topologically trivial [10], then the topological phase featured with the $\mathbb{Z}_2$ invariant appears [35]. Note that the quantization mechanism of TRS associated with an imaginary-line gap is the same as that of PHS† associated with a real-line gap, due to the unification of TRS and PHS† [36].

Specific examples. Here, we present two simple models (with two sites per unit cell) to provide numerical evidence for some of the results obtained above. First, let us consider a bipartite lattice where electrons are subject to a NH Su-Schrieffer-Heeger (SSH) Hamiltonian, that exhibits NH polarization due to the presence of SLS. The Hamiltonian reads

$$\hat{H} = \sum_j [v(\hat{a}_j^\dagger \hat{b}_j - \hat{b}_j^\dagger \hat{a}_j) + w(\hat{a}_j^\dagger \hat{b}_{j-1} + \hat{b}_{j-1}^\dagger \hat{a}_j)], \tag{5}$$

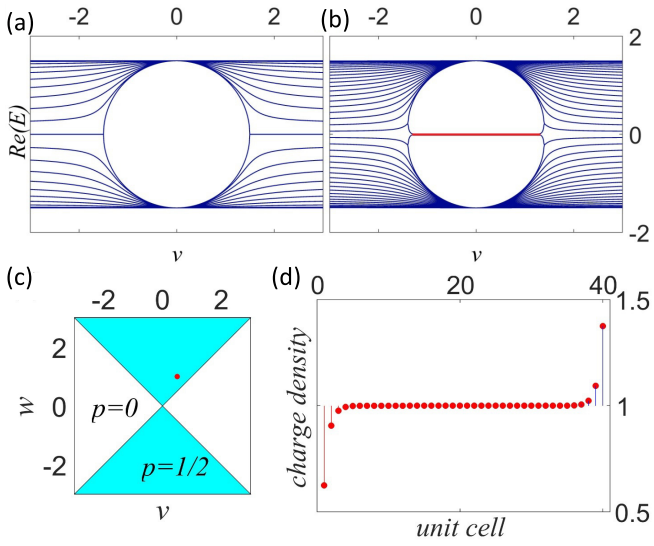

FIG. 2. The real part of the eigenvalues of the NH Hamiltonian defined in Eq. (5), when $w = 1.5, N = 40$, and $v \in (-3, 3)$, obtained for (a) periodic and (b) open boundary conditions, respectively. Their imaginary parts are plotted in the SM [42]. The red line in (b) marks the zero-energy edge modes. (c) The polarization phase diagram as functions of $w, v \in (-3, 3)$. (d) Electron charge distribution in the topologically nontrivial polarization phase for $w = 1.0, v = 0.5$ [i.e., the red dot denoted in (c)]. The total electron charge at the ends is $\pm e/2$ relative to background.

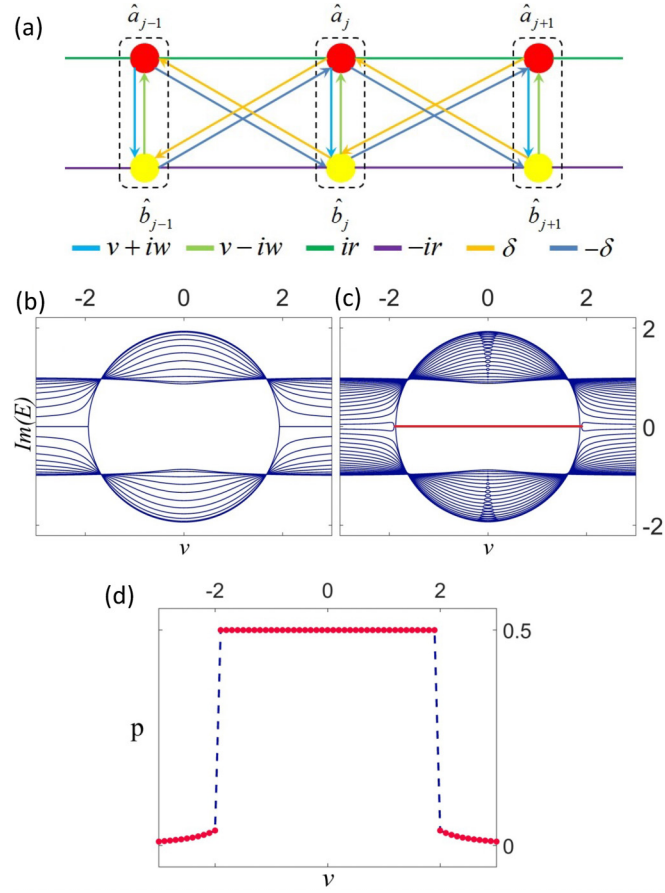

FIG. 3. NH polarization and TRS symmetry. (a) Schematic of a one-dimensional NH lattice which obeys only TRS. The dashed boxes indicate the unit cells. (b), (c) Associated imaginary energy spectra, when $w = 0.5, r = 1.0, \delta = 0.5, N = 40$, and $v \in (-3, 3)$ [see Eq. (6)], computed for (a) periodic and (b) open boundary conditions, respectively. Their real parts are plotted in the SM [42]. The red line in (b) marks the zero-energy edge modes. The energy spectrum presents an imaginary energy gap for $|v| \leqslant \sqrt{4r^2 - w^2}$. (d) Numerical values of the polarization p as a function of v, for the same parameters as in (b) and (c).

where $\hat{a}_j$ ($\hat{a}_j^\dagger$) and $\hat{b}_j$ ($\hat{b}_j^\dagger$) are annihilation (creation) operators on sites A and B of the jth cell, respectively, and $v, w \in \mathbb{R}$ denote hopping amplitudes. In this model, the non-Hermiticity is induced through the opposite sign (v and $-v$) of $a \to b$ and $b \to a$ tunnelings within a unit cell. A Hamiltonian such as the one in Eq. (5) can be effectively realized in photonic simulators, where asymmetric couplings are obtained by tailoring gains and losses of individual optical modes, encoding the lattice sites of our model [56]. The Hamiltonian in Eq. (5) obeys SLS and TRS, with the corresponding operators $S = \oplus_{j=1}^{N} \sigma_z$ and $T = \oplus_{j=1}^{N} \sigma_0$, where σ_0 and σ_z are the identity matrix and Pauli matrix, respectively. These symmetries force the eigenenergies to come in $(E, -E^*)$ pairs, thus presenting a real-line gap in the energy spectrum [see Figs. 2(a) and 2(b); the complete spectrum is given in Sec. VIII of SM [42]]. By means of the NH polarization formula reported in Eq. (3), the topological phase diagram is computed as functions of w and v [see Fig. 2(c)], which clearly presents trivial and nontrivial phases that are separated by lines $|w| = |v|$. In addition, the charge density distribution for the case $w = 1.0$, $v = 0.5$, $N = 40$ [i.e., the red dot in Fig. 2(c)] is plot in Fig. 2(d), indicating the validity of conventional BBC (see Sec. VIII of SM [42]). Note that the quantized NH polarization is protected by SLS, though this model also obeys TRS. The latter is responsible for polarization quantization only when an imaginary-line gap is present (see Table I). Let us stress that in finite lattices, we compute the polarization in terms of real-valued Wannier centers. To do so, singular value decomposition [57] is used to construct numerical Wilson-loop operators [42].

The second model is schematically shown in Fig. 3(a), whose Hamiltonian in momentum space reads

$$H(k) = [v + 2i\delta \sin(k)]\sigma_x + w\sigma_y + 2ir\cos(k)\sigma_z, \quad (6)$$

where $(\sigma_x, \sigma_y, \sigma_z)$ are Pauli matrices. It is easy to verify that the Hamiltonian in Eq. (6) obeys only TRS with $T = \sigma_x$, and the energy spectrum presents an imaginary-line gap for $|v| \leqslant \sqrt{4r^2 - w^2}$, as shown in Figs. 3(b) and 3(c), while for $|v| \geqslant \sqrt{4r^2 - w^2}$ there is a real-line gap [42]. Table I reveals that only in the presence of an imaginary-line gap does TRS quantize NH polarization, as shown in Fig. 3(d) for $|v| \leqslant \sqrt{4r^2 - w^2}$. Contrarily, the NH polarization in the range $|v| \geqslant \sqrt{4r^2 - w^2}$ deviates from the quantized value $p = 0$ due to the presence of a real-line gap in this range.

Conclusions. In summary, we proposed a complete theory for the electric polarization in 1D NH systems presenting line-gapped spectra, and obtained the associated quantization conditions, which are found to be more than those of the Hermitian case. This is essentially related to the possibility

that the gap type of line-gapped NH systems may be real or imaginary. We plan to extend these studies to superconducting chains [58] and high-order topological multipole moments [59–69], whose definition in NH systems looks feasible by using the same approach presented here. Although the present Letter focuses on the case of independent electrons, Resta's formula was devised for many-particle interacting systems [5], so another potential followup of our work is to calculate the electric polarization of NH systems, where many-body effects are included.

Acknowledgments. We appreciate fruitful discussions with Dr. K. Kawabata, Profs. Z. Wang, S. Longhi, Dr. A. Dauphin, Profs. P. Massignan, E. J. Bergholtz, and M. Nakamura. J.H. is thankful for financial support from the National Natural Science Foundation of China (No. 61805141), J.H., L.M., and F.C. acknowledge financial support from the European Union Horizon 2020 program, under European Research Council (ERC) Grant No. 694683 (PHOSPhOR). G.D.F., L.M., and F.C. acknowledge financial support from PNRR MUR Project No. PE0000023-NQSTI.

[1] S. Baroni, P. Giannozzi, and A. Testa, Green's-Function Approach to Linear Response in Solids, Phys. Rev. Lett. **58**, 1861 (1987).
[2] R. Resta, Theory of the electric polarization in crystals, Ferroelectrics **136**, 51 (1992).
[3] R. D. King-Smith and D. Vanderbilt, Theory of polarization of crystalline solids, Phys. Rev. B **47**, 1651(R) (1993).
[4] R. Resta, Macroscopic polarization in crystalline dielectrics: The geometric phase approach, Rev. Mod. Phys. **66**, 899 (1994).
[5] R. Resta, Quantum-Mechanical Position Operator in Extended Systems, Phys. Rev. Lett. **80**, 1800 (1998).
[6] N. Marzari, A. A. Mostofi, J. R. Yates, I. Souza, and D. Vanderbilt, Maximally localized Wannier functions: Theory and applications, Rev. Mod. Phys. **84**, 1419 (2012).
[7] J. Zak, Berry's Phase for Energy Bands in Solids, Phys. Rev. Lett. **62**, 2747 (1989).
[8] M. V. Berry, Quantal phase factors accompanying adiabatic changes, Proc. R. Soc. London, Ser. A **392**, 45 (1984).
[9] D. Xiao, M.-C. Chang, and Q. Niu, Berry phase effects on electronic properties, Rev. Mod. Phys. **82**, 1959 (2010).
[10] W. A. Benalcazar, B. A. Bernevig, and T. L. Hughes, Electric multipole moments, topological multipole moment pumping, and chiral hinge states in crystalline insulators, Phys. Rev. B **96**, 245115 (2017).
[11] Y. Hatsugai, Chern Number and Edge States in the Integer Quantum Hall Effect, Phys. Rev. Lett. **71**, 3697 (1993).
[12] Z. Wang, Y. Chong, J. D. Joannopoulos, and M. Soljačić, Observation of unidirectional backscattering-immune topological electromagnetic states, Nature (London) **461**, 772 (2009).
[13] Z. Wang, Y. D. Chong, J. D. Joannopoulos, and M. Soljačić, Reflection-Free One-Way Edge Modes in a Gyromagnetic Photonic Crystal, Phys. Rev. Lett. **100**, 013905 (2008).
[14] C. M. Bender, D. C. Brody, and H. F. Jones, Complex Extension of Quantum Mechanics, Phys. Rev. Lett. **89**, 270401 (2002).
[15] Z. Lin, H. Ramezani, T. Eichelkraut, T. Kottos, H. Cao, and D. N. Christodoulides, Unidirectional Invisibility Induced by $\mathcal{PT}$-Symmetric Periodic Structures, Phys. Rev. Lett. **106**, 213901 (2011).
[16] A. Regensburger, C. Bersch, M.-A. Miri, G. Onishchukov, D. N. Christodoulides, and U. Peschel, Parity–time synthetic photonic lattices, Nature (London) **488**, 167 (2012).
[17] B. Peng, K. Özdemir, Ş, F. Lei, F. Monifi, M. Gianfreda, G. L. Long, S. Fan, F. Nori, C. M. Bender, and L. Yang, Parity–time-symmetric whispering-gallery microcavities, Nat. Phys. **10**, 394 (2014).
[18] T. Gao *et al.*, Observation of non-Hermitian degeneracies in a chaotic exciton-polariton billiard, Nature (London) **526**, 554 (2015).
[19] J. Doppler, A. A. Mailybaev, J. Böhm, U. Kuhl, A. Girschik, F. Libisch, T. J. Milburn, P. Rabl, N. Moiseyev, and S. Rotter, Dynamically encircling an exceptional point for asymmetric mode switching, Nature (London) **537**, 76 (2016).
[20] J. W. Yoon *et al.*, Time-asymmetric loop around an exceptional point over the full optical communications band, Nature (London) **562**, 86 (2018).
[21] J. Wiersig, Enhancing the Sensitivity of Frequency and Energy Splitting Detection by Using Exceptional Points: Application to Microcavity Sensors for Single-Particle Detection, Phys. Rev. Lett. **112**, 203901 (2014).
[22] Liu, Z.-P., J. Zhang, K. Özdemir, Ş, B. Peng, H. Jing, X.-Y. Lü, C.-W. Li, L. Yang, F. Nori, and Y.-x. Liu, Metrology with $\mathcal{PT}$-Symmetric Cavities: Enhanced Sensitivity near the $\mathcal{PT}$-Phase Transition, Phys. Rev. Lett. **117**, 110802 (2016).
[23] H.-K. Lau and A. A. Clerk, Fundamental limits and non-reciprocal approaches in non-Hermitian quantum sensing, Nat. Commun. **9**, 4320 (2018).
[24] S. Yao and Z. Wang, Edge States and Topological Invariants of Non-Hermitian Systems, Phys. Rev. Lett. **121**, 086803 (2018).
[25] N. Okuma, K. Kawabata, K. Shiozaki, and M. Sato, Topological Origin of Non-Hermitian Skin Effects, Phys. Rev. Lett. **124**, 086801 (2020).
[26] K. Zhang, Z. Yang, and C. Fang, Correspondence between Winding Numbers and Skin Modes in Non-Hermitian Systems, Phys. Rev. Lett. **125**, 126402 (2020).
[27] Y. Yi and Z. Yang, Non-Hermitian Skin Modes Induced by On-Site Dissipations and Chiral Tunneling Effect, Phys. Rev. Lett. **125**, 186802 (2020).
[28] L. Feng, Y.-L. Xu, W. S. Fegadolli, M.-H. Lu, J. E. Oliveira, V. R. Almeida, Y.-F. Chen, and A. Scherer, Experimental demonstration of a unidirectional reflectionless parity-time metamaterial at optical frequencies, Nat. Mater. **12**, 108 (2013).
[29] B. Zhen, C. W. Hsu, Y. Igarashi, L. Lu, I. Kaminer, A. Pick, S.-L. Chua, J. D. Joannopoulos, and M. Soljačić, Spawning rings of exceptional points out of Dirac cones, Nature (London) **525**, 354 (2015).
[30] H. Hodaei, A. U. Hassan, S. Wittek, H. Garcia-Gracia, R. El-Ganainy, D. N. Christodoulides, and M. Khajavikhan, Enhanced sensitivity at higher-order exceptional points, Nature (London) **548**, 187 (2017).

[31] L. Xiao, T. Deng, K. Wang, G. Zhu, Z. Wang, W. Yi, and P. Xue, Non-Hermitian bulk–boundary correspondence in quantum dynamics, Nat. Phys. **16**, 761 (2020).

[32] E. Lee, H. Lee, and B.-J. Yang, Many-body approach to non-Hermitian physics in fermionic systems, Phys. Rev. B **101**, 121109 (2020).

[33] C. Ortega-Taberner, L. Rødland, and M. Hermanns, Polarization and entanglement spectrum in non-Hermitian systems, Phys. Rev. B **105**, 075103 (2022).

[34] S. Masuda and M. Nakamura, Relationship between the electronic polarization and the winding number in non-Hermitian systems, J. Phys. Soc. Jpn. **91**, 043701 (2022).

[35] K. Kawabata, K. Shiozaki, M. Ueda, and M. Sato, Symmetry and Topology in Non-Hermitian Physics, Phys. Rev. X **9**, 041015 (2019).

[36] K. Kawabata, S. Higashikawa, Z. Gong, Y. Ashida, and M. Ueda, Topological unification of time-reversal and particle-hole symmetries in non-Hermitian physics, Nat. Commun. **10**, 297 (2019).

[37] G. H. Wannier, Dynamics of band electrons in electric and magnetic fields, Rev. Mod. Phys. **34**, 645 (1962).

[38] P. Comaron, V. Shahnazaryan, W. Brzezicki, T. Hyart, and M. Matuszewski, Non-Hermitian topological end-mode lasing in polariton systems, Phys. Rev. Res. **2**, 022051 (2020).

[39] H. Hu and E. Zhao, Knots and Non-Hermitian Bloch Bands, Phys. Rev. Lett. **126**, 010401 (2021).

[40] X.-W. Luo and C. Zhang, Higher-Order Topological Corner States Induced by Gain and Loss, Phys. Rev. Lett. **123**, 073601 (2019).

[41] F. K. Kunst, E. Edvardsson, J. C. Budich, and E. J. Bergholtz, Biorthogonal Bulk-Boundary Correspondence in Non-Hermitian Systems, Phys. Rev. Lett. **121**, 026808 (2018).

[42] See Supplemental Material at http://link.aps.org/supplemental/10.1103/PhysRevB.107.L121101 for more details on the derivations supporting our theoretical results and on the models used for numerical calculations.

[43] R. Resta, M. Posternak, and A. Baldereschi, Towards a Quantum Theory of Polarization in Ferroelectrics: The Case of $KNbO_3$, Phys. Rev. Lett. **70**, 1010 (1993).

[44] D. Vanderbilt and R. King-Smith, Electric polarization as a bulk quantity and its relation to surface charge, Phys. Rev. B **48**, 4442 (1993).

[45] D. C. Brody, Biorthogonal quantum mechanics, J. Phys. A: Math. Theor. **47**, 035305 (2013).

[46] M. Hafezi, E. A. Demler, M. D. Lukin, and J. M. Taylor, Robust optical delay lines with topological protection, Nat. Phys. **7**, 907 (2011).

[47] M. Hafezi, S. Mittal, J. Fan, A. Migdall, and J. Taylor, Imaging topological edge states in silicon photonics, Nat. Photonics **7**, 1001 (2013).

[48] H. Shen, B. Zhen, and L. Fu, Topological Band Theory for Non-Hermitian Hamiltonians, Phys. Rev. Lett. **120**, 146402 (2018).

[49] S. Mittal, V. V. Orre, G. Zhu, M. A. Gorlach, A. Poddubny, and M. Hafezi, Photonic quadrupole topological phases, Nat. Photonics **13**, 692 (2019).

[50] J. K. Ashóth, L. Oroszlány, and A. Pályi, *A Short Course on Topological Insulators*, Lecture Notes in Physics, Vol. 919 (Springer, Berlin, 2016).

[51] E. V. F. de Aragão, D. Moreno, S. Battaglia, G. L. Bendazzoli, S. Evangelisti, T. Leininger, N. Suaud, and J. A. Berger, A simple position operator for periodic systems, Phys. Rev. B **99**, 205144 (2019).

[52] W. H. Press, S. A. Teukolsky, W. T. Vetterling, and B. P. Flannery, *Numerical Recipes in Fortran 90: The Art of Parallel Scientific Computing* (Cambridge University Press, Cambridge, UK, 1996).

[53] A. Alexandradinata, X. Dai, and B. A. Bernevig, Wilson-loop characterization of inversion-symmetric topological insulators, Phys. Rev. B **89**, 155114 (2014).

[54] M. L. N. Chen, L. J. Jiang, S. Zhang, R. Zhao, Z. Lan, and W. E. I. Sha, Comparative study of Hermitian and non-Hermitian topological dielectric photonic crystals, Phys. Rev. A **104**, 033501 (2021).

[55] S. Lieu, Topological phases in the non-Hermitian Su-Schrieffer-Heeger model, Phys. Rev. B **97**, 045106 (2018).

[56] S. Weidemann, M. Kremer, T. Helbig, T. Hofmann, A. Stegmaier, M. Greiter, R. Thomale, and A. Szameit, Topological funneling of light, Science **368**, 311 (2020).

[57] I. Souza, N. Marzari, and D. Vanderbilt, Maximally localized Wannier functions for entangled energy bands, Phys. Rev. B **65**, 035109 (2001).

[58] A. Maiellaro, F. Romeo, C. A. Perroni, V. Cataudella, and R. Citro, Unveiling signatures of topological phases in open Kitaev chains and ladders, Nanomaterials **9**, 894 (2019).

[59] W. A. Benalcazar, B. A. Bernevig, and T. L. Hughes, Quantized electric multipole insulators, Science **357**, 61 (2017).

[60] B. Bradlyn, L. Elcoro, J. Cano, M. Vergniory, Z. Wang, C. Felser, M. I. Aroyo, and B. A. Bernevig, Topological quantum chemistry, Nature (London) **547**, 298 (2017).

[61] F. Schindler, A. M. Cook, M. G. Vergniory, Z. Wang, S. S. Parkin, B. A. Bernevig, and T. Neupert, Higher-order topological insulators, Sci. Adv. **4**, eaat0346 (2018).

[62] S. Imhof *et al.*, Topolectrical-circuit realization of topological corner modes, Nat. Phys. **14**, 925 (2018).

[63] M. Serra-Garcia, V. Peri, R. Süsstrunk, O. R. Bilal, T. Larsen, L. G. Villanueva, and S. D. Huber, Observation of a phononic quadrupole topological insulator, Nature (London) **555**, 342 (2018).

[64] C. W. Peterson, W. A. Benalcazar, T. L. Hughes, and G. Bahl, A quantized microwave quadrupole insulator with topologically protected corner states, Nature (London) **555**, 346 (2018).

[65] H. Xue, Y. Yang, F. Gao, Y. Chong, and B. Zhang, Acoustic higher-order topological insulator on a kagome lattice, Nat. Mater. **18**, 108 (2019).

[66] Y. Wang *et al.*, Quantum superposition demonstrated higher-order topological bound states in the continuum, Light: Sci. Appl. **10**, 173 (2021).

[67] L. Luo, H.-X. Wang, Z.-K. Lin, B. Jiang, Y. Wu, F. Li, and J.-H. Jiang, Observation of a phononic higher-order Weyl semimetal, Nat. Mater. **20**, 794 (2021).

[68] S. A. A. Ghorashi, T. Li, M. Sato, and T. L. Hughes, Non-Hermitian higher-order Dirac semimetals, Phys. Rev. B **104**, L161116 (2021).

[69] S. A. A. Ghorashi, T. Li, and M. Sato, Non-Hermitian higher-order Weyl semimetals, Phys. Rev. B **104**, L161117 (2021).